OPEN ACCESS
IOP Publishing
Journal of Physics G: Nuclear and Particle Physics
J. Phys. G: Nucl. Part. Phys. **50** (2023) 045110 (12pp)
https://doi.org/10.1088/1361-6471/acbece

Proton-neutron entanglement in the nuclear shell model

Calvin W Johnson* **and Oliver C Gorton**

San Diego State University, 5500 Campanile Drive, San Diego, CA 92182-1233, United States of America

E-mail: cjohnson@sdsu.edu

Received 30 November 2022, revised 20 February 2023
Accepted for publication 24 February 2023
Published 17 March 2023

Abstract

We compute the proton-neutron entanglement entropy in the interacting nuclear shell model for a variety of nuclides and interactions. Some results make intuitive sense, for example, that the shell structure, as governed by single-particle and monopole energies, strongly affects the energetically available space and thus the entanglement entropy. We also find a surprising result: that the entanglement entropy at low excitation energy tends to decrease for nuclides when $N \neq Z$. While we provide evidence this arises from the physical nuclear force by contrasting with random two-body interactions which shows no such decrease, the exact mechanism is unclear. Nonetheless, the low entanglement suggests that in models of neutron-rich nuclides, the coupling between protons and neutrons may be less computationally demanding than one might otherwise expect.

Keywords: nuclear, shell model, entanglement

(Some figures may appear in colour only in the online journal)

1. Introduction

The structure of atomic nuclei exhibits a mixture of simple and complex behaviors. What is meant by 'simple' can be subtle, but typically it means the behavior can be described by far fewer degrees of freedom than that required by modeling the nucleus as a collection of A interacting nucleons; examples of simplicity include algebraic models [1] and mean-field

* Author to whom any correspondence should be addressed.

pictures [2]. Of course, one must acknowledge that models themselves are not physical observables. Furthermore, complex models can mimic simpler ones, for example quasidynamic symmetries [3–5], where a Hamiltonian mixes symmetries yet observables such as spectra and ratios of transition strengths are consistent with 'simpler' symmetry-respecting models.

Entanglement is a concept describing whether the observable coordinates of a quantum system are independent; whether measurement of one generalized coordinate q_1 influences future measurements of another coordinate q_2 of a system $\psi(q_1, q_2, \ldots)$ [6, 7]. Such correlations can be described by the entanglement entropy, a concept which has become popular in recent years due to increasing interest in quantum information and the potential of quantum computing [8, 9]. It is trivial to write down states which are either separable (not entangled) or in a superposition of separable states (entangled), but the creation of entangled states in nature relies on the existence of an interaction that mixes the relevant degrees of freedom.

Here we consider the entanglement between the proton components and neutron components of configuration-interaction models of nuclei. Other recent work in entanglement entropy in nuclei addressed single-particle and seniority-mode entanglement [10, 11] as well as orbital entanglement revealing shell closures [12]; we note the first two papers reference unpublished versions of the research reported here.

Although it does not directly correspond to the work here, we point out previous analyses of nuclear configuration-interaction wave functions using 'entropy,' such as the configuration information entropy [13, 14], which is simple but basis dependent, and the invariant correlation entropy [15], which is much more complicated to compute. By contrast, because of the way our configuration-interaction code constructs the wave functions, extraction of the wave function amplitudes in terms of proton-neutron coefficients is straightforward, a significant motivation for our approach.

In section 2 we lay out the basic framework of shell model configuration-interaction calculations. In section 3, we define entanglement entropy as well as related concepts. We then provide examples of entanglement entropies for a variety of cases and show how much of the behavior for ground state entropies can be understood through standard concepts in nuclear structure physics. A persistent phenomenon, however, is not so easily explained: realistic ground states of nuclides with $N \neq Z$ tend to have significantly smaller entanglement entropies than those with $N = Z$. We also show trends for entropies for all states. We can show this is related to some components of realistic nuclear forces by contrasting them with results using random interactions. While the mechanism for suppressing the entanglement eludes us, it is nonetheless worth reporting, not only as an apparently robust yet unexplained phenomenon but also because it has a practical consequence: the low-lying states of neutron-rich nuclides have fewer nontrivial correlations between the proton and neutron components. This, in turn, suggests a practical approach for such nuclides, one which we are currently developing.

2. The nuclear configuration-interaction shell model

We find low-lying states of a nuclear Hamiltonian by the configuration-interaction method in a shell model basis [16–18]. Any many-body Hamiltonian can be written in second quantization formalism as a polynomial in creation and annihilation operators [2]:

$$\hat{H} = \sum_i \epsilon_i \hat{a}_i^\dagger \hat{a}_i + \frac{1}{4}\sum_{ijkl} V_{ijkl} \hat{a}_i^\dagger \hat{a}_j^\dagger \hat{a}_l \hat{a}_k, \tag{1}$$

where ϵ_i are single-particle energies and V_{ijkl} are the two-body interaction matrix elements. The single-particle operators $\hat{a}_i^\dagger$ create spin-$1/2$ nucleons in simple harmonic oscillator states with quantum numbers: n_i (radial quantum number), l_i (orbital angular momentum), and j_i (total angular momentum). Many-body states are constructed as antisymmetrized products of these single-particle states.

To make calculations tractable, we limit the number of single-particle valence states. For example, several of our calculations assume a fixed ^{16}O core and allow valence nucleons in the $1s_{1/2}$-$0d_{3/2}$-$0d_{5/2}$ orbits, colloquially known as the *sd*-shell; we also work in the *pf*-shell (^{40}Ca core with valence orbits $1p_{1/2,3/2}$-$0f_{5/2,7/2}$) and the combined *sd-pf* shells. Starting from a finite single-particle valence space yields a finite many-body basis [18]:

$$|\Psi\rangle = \sum_\alpha c_\alpha |\alpha\rangle, \tag{2}$$

where we use the occupation representation of Slater determinants, that is, of the form $|\alpha\rangle = \prod_i \hat{a}_i^\dagger |0\rangle$. In particular, we work in the *M*-scheme, which means the total J_z or M of each basis state is fixed to the same value. For our calculations here we construct all possible valence configurations with fixed M. Furthermore, we factorize the basis into proton (π) and neutron (ν) components, so that we can write:

$$|\alpha\rangle = |\mu_\pi\rangle \otimes |\sigma_\nu\rangle. \tag{3}$$

This enables calculation of the proton-neutron entanglement entropy.

The parameters ϵ_i and V_{ijkl} in equation (1) are input parameters of the Hamiltonian. For details see the reviews in [16–18]. For our calculations, we used high-quality empirical interactions fitted separately in each model space to experimental spectra, schematic interactions known to capture many features of nuclear structure, and randomly generated interactions. Using equation (1) and the factorized basis (2) one can compute [18, 19] the matrix elements of the Hamiltonian in the many-body basis, $H_{\alpha,\beta} = \langle\alpha|\hat{H}|\beta\rangle$. Then the time-independent Schrödinger equation becomes a simple matrix eigenvalue problem: $\mathbf{H}\vec{c} = E\vec{c}$.

3. Entanglement entropy

The entanglement entropy is a fundamental tool in quantum information science [6, 8, 9]. Here we briefly review the development found in those sources.

For a pure quantum state $|\Psi\rangle$, the density operator is $\hat{\rho} = |\Psi\rangle\langle\Psi|$; in a basis $\{|\alpha\rangle\}$, i.e. equation (2), the density matrix elements are $\rho_{\alpha'\alpha} = c'_\alpha c^*_\alpha$. Because this is idempotent, $\rho^2 = \rho$, and thus has either 0 or 1 as eigenvalues, the von Neumann entropy, $S = -\mathrm{tr}(\rho \log \rho)$ vanishes.

Suppose we work in a bipartite Hilbert space, e.g. $\mathcal{H} = \mathcal{H}_\pi \otimes \mathcal{H}_\nu$, with basis states such as (3); we can then write equation (2) explicitly as

$$|\Psi\rangle = \sum_{\mu,\sigma} c_{\mu,\sigma} |\mu_\pi\rangle \otimes |\sigma_\nu\rangle. \tag{4}$$

An unentangled state is one where one can transform to a basis where the amplitudes are separable, that is $c_{\mu,\sigma} = a_\mu b_\sigma$; in this case the state could be written as a simple product: $|\Psi\rangle = (\sum_\mu a_\mu |\mu_\pi\rangle) \otimes (\sum_\sigma b_\sigma |\sigma_\nu\rangle)$. States which do not satisfy this are entangled.

In the basis (4) the density matrix is $\rho_{\mu'\sigma',\mu\sigma} = c_{\mu'\sigma'} c^*_{\mu\sigma}$. This density matrix is idempotent. To get the *reduced* density matrix, one traces over one of the subspace indices:

$$\rho^{\rm red}_{\mu',\mu} = \sum_{\sigma} c_{\mu'\sigma} c^*_{\mu\sigma}. \tag{5}$$

If the state is unentangled, the reduced density matrix will also be idempotent. For a general state the reduced density matrix need not be idempotent, and its eigenvalues can be between 0 and 1. Then the entanglement entropy [6]

$$S_{\rm entangled} = -{\rm tr}\ \rho^{\rm red} \ln \rho^{\rm red}, \tag{6}$$

can be nonzero. Because unentangled states must have zero entanglement entropy, nonzero entropy is a measure of entanglement [6]. The fact that the eigenvalues of $\rho^{\rm red}$ are real and non-negative, and independent of which subspace index we trace over, is a result of the singular-value decomposition theorem; this is also called the Schmidt decomposition, especially in quantum information science. The maximum entropy possible is the natural logarithm of the smaller subspace dimensions,

$$S_{\rm max} = \ln(\min(\dim_\pi, \dim_\nu)). \tag{7}$$

Because our code is written using an explicit proton-neutron basis, it is easy to extract $c_{\mu,\sigma}$ for any calculated state and then compute the entanglement entropy.

4. Results

We work in three different model spaces and with several different shell model interactions. All of our calculations are in the M-scheme, that is, a basis with fixed total J_z. We start with several studies of $N = Z$ nuclides in the *sd*-shell, where our results can be easily understood. We then look at cases in the *sd*, *pf*, and *sd-pf* spaces with $N \neq Z$, which leads to a surprise: ground states with $N \neq Z$ have significantly lower entanglement entropies than those with $N = Z$. By comparing with randomly generated interactions we provide evidence that this phenomenon has its origin in physical forces; but beyond that, we have yet to understand the specific mechanism. Finally, we look at the behavior of the entropy over the entire spectrum.

4.1. Examples with $N = Z$ and the role of the shell structure

In this subsection we discuss some introductory results, focusing on $N = Z$ nuclides.

Our first examples in figure 1 are the ground state entanglement entropies for $N = Z$ nuclides in the so-called *sd*-shell, which has a fixed ^{16}O core and valence particles in the $1s_{1/2}$-$0d_{3/2}$-$0d_{5/2}$ orbitals. For convenience, we give the $M = 0$ dimensions in table 1. Here the proton and neutron many-body spaces have equal dimensions. We use a high-quality empirical interaction, the universal *sd*-shell interaction, version B or USDB, which, like all similar empirical interactions, is represented as a list of single-particle energies and two-body matrix elements fitted to data [20]. We also show in figure 1(a) the entropies for ground states of the attractive isoscalar quadrupole–quadrupole (QQ) interaction, the attractive isovector (IV) pairing, that is, nucleons paired up to isospin $T = 1$, and the attractive isoscalar (IS) pairing, or nucleons paired up to $T = 0$.

These schematic interactions are well-known in nuclear structure physics [2, 16, 25]; we give their exact definitions in the appendix. Unsurprisingly, isoscalar pairing, which forces protons to pair with neutrons, has nearly maximal entanglement entropy. Isovector pairing shows a strong odd–even effect: odd–odd nuclides, where at least one proton and at least one neutron must pair up, has much higher entropy than the even–even cases. Ground states of the QQ interaction have a much weaker odd–even staggering, while USDB ground states have the lowest entropies of all and exhibit no odd–even staggering.

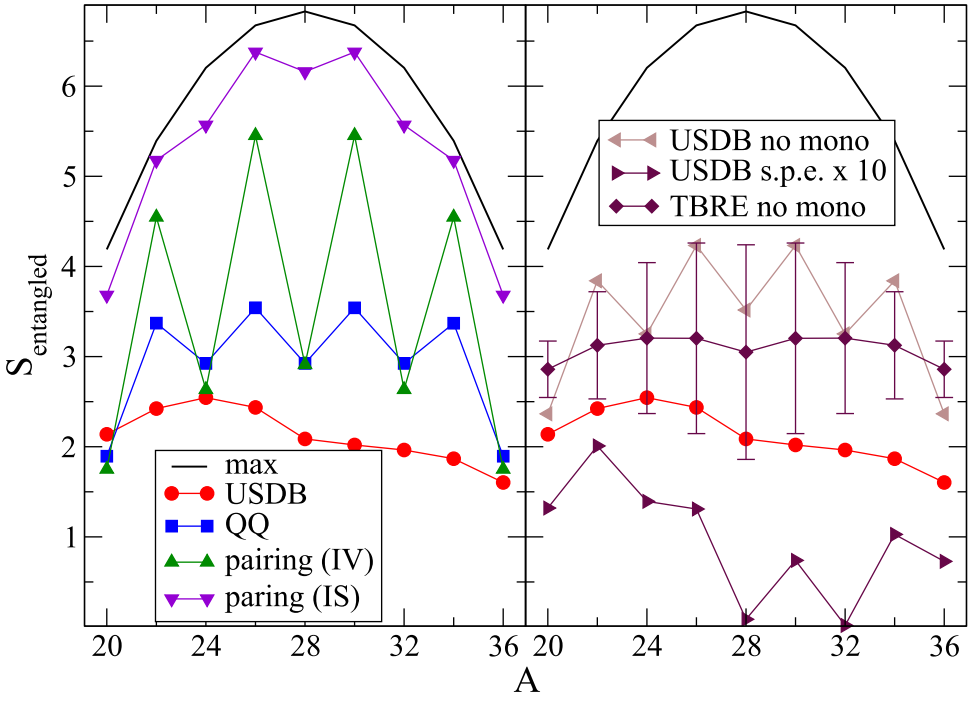

Figure 1. Ground state entanglement entropy for $N = Z$ nuclides in the *sd*-shell. Both panels show results for USDB [20], a high-quality empirical interaction, and the maximum possible entanglement entropy. In panel (a)we show results for an attractive isoscalar quadrupole–quadrupole ('QQ') interaction; isovector (IV) and isoscalar (IS) pairing. In panel (b) we show results for USDB with single-particle energies and monopole interactions which have been set to zero, eliminating shell structure ('no mono'), and with single-particle energies inflated by a factor of ten, amplifying shell structure ('s.p.e. x 10'). Additionally, panel (b) gives the average and standard deviation for calculations drawn from a two-body random ensemble [21], also with shell structure eliminated ('TBRE no mono'). See text for discussion.

Table 1. $M = 0$ dimensions for the $N = Z$ nuclides in figure 1 with valence nucleons in the *sd*-shell. Because there are a maximum of 12 valence nucleons of either species, the dimensions have a particle-hole symmetry around N, Z = 14.

Nuclide	dimension
^{20}Ne, ^{36}Ar	640
^{22}Na, ^{34}Cl	6116
^{24}Mg, ^{32}S	28 503
^{26}Al, ^{30}P	69 784
^{28}Si	93 710

In figure 1(b), we further investigate the origin of some of these behaviors. The shell structure of nuclei is governed by the single-particle energies and the so-called monopole terms [18], that is, terms in the interaction of the form $\hat{n}_a\hat{n}_b$ where $\hat{n}_a$ is the number operator for orbital a. By setting the single-particle energies and monopole terms to zero, the ground state entanglement entropy increases, and shows an odd–even staggering comparable to QQ.

Conversely, by inflating the standard USDB values of the single-particle energies ($\epsilon(1s_{1/2}) = -3.2079$ MeV, $\epsilon(0d_{3/2}) = 2.1117$ MeV, and $\epsilon(0d_{5/2}) = -3.9257$ MeV) by a factor of 10, we restrict the space energetically available and dramatically decrease the ground state entanglement entropy, reaching zero at shell closures. Finally, we considered two-body interactions drawn from a random ensemble (TBRE [21]), also removing single-particle energies and monopole terms We used results from ten different members of the ensemble to get average entropies and corresponding standard deviations. From this, we learn that, first, the shell structure, as encoded in single-particle energies and monopole terms, has a strong effect on the entanglement entropy, by energetically restricting the available model space and thus reducing the effective dimension. While the 'no mono' USDB results appear consistent with a randomly drawn interaction, it does show a nontrivial odd–even staggering. Later, we will see additional behaviors that strongly differ between USDB and randomly generated interactions.

From these numerical experiments we conclude the lower entanglement of the full USDB wave functions is due to the shell structure, i.e. the monopole terms and single-particle energies. We speculate the lack of odd–even staggering in the entropies of full USDB calculations may be due to many small, quasi-random components in the interaction beyond pairing and QQ.

4.2. Away from $N = Z$

In the previous subsection we considered exclusively nuclides with $N = Z$. Here we compare entropies for nuclides with $N \neq Z$, and find systematically lower entropies–albeit when using physical forces. Because we use interactions that respect isospin as a good symmetry, we only consider here $N > Z$.

In figure 2 we compare the ground state entropies for 'triplets' of nuclides. These triplets are set in the same valence space, either *sd* or *pf*, and all members of a triplet have the same number of valence protons or proton holes, and the same number of valence neutrons or neutron holes. For example, we have ^{20}Ne, with 2 valence protons and 2 valence neutrons; ^{36}Ar, with 2 proton holes and 2 neutron holes (since the filled *sd* valence orbitals contain 12 particles of a given nuclear species); and ^{28}Ne, with 2 valence protons and 2 neutron holes. By this construction, all members of a triplet have exactly the same dimensionalities. For the *sd*-shell cases in figure 2(a), following figure 1, we compare entanglement entropies from ground states computed with the full USDB interaction, USDB with monopole terms and single-particle energies set to zero, and finally entropies of ground states calculated from the two-body random ensemble (with monopole terms zeroed out). For the *pf*-shell cases in figure 2(b), we do the same but replace USDB with the GX1A interaction [24].

We see a strong and persistent trend: ground states of nuclides with $N \neq Z$ computed with realistic interactions have significantly lower entanglement than those with $N = Z$, a result we have replicated in other shell model spaces we do not show. To put this in perspective, an entropy difference of 1 corresponds to a difference in effective dimensionality of $e = 2.71\ldots$. This trend is stronger for even–even nuclides and when the shell structure is removed. For ground states computed under the TBRE, however, that trend disappears and is even slightly reversed. While we have made attempts to devise a plausible model for these behaviors, for example why the $N \neq Z$ entropy is lower for realistic interactions but is higher for the TBRE, we have not succeeded.

Because this trend suggests a lower entanglement for neutron-rich nuclides (or, because of isospin symmetry for these interactions, proton-rich as well), we continue our investigation in figure 3, where we consider cross-shell examples in the *sd-pf* space using the 'mu-db'

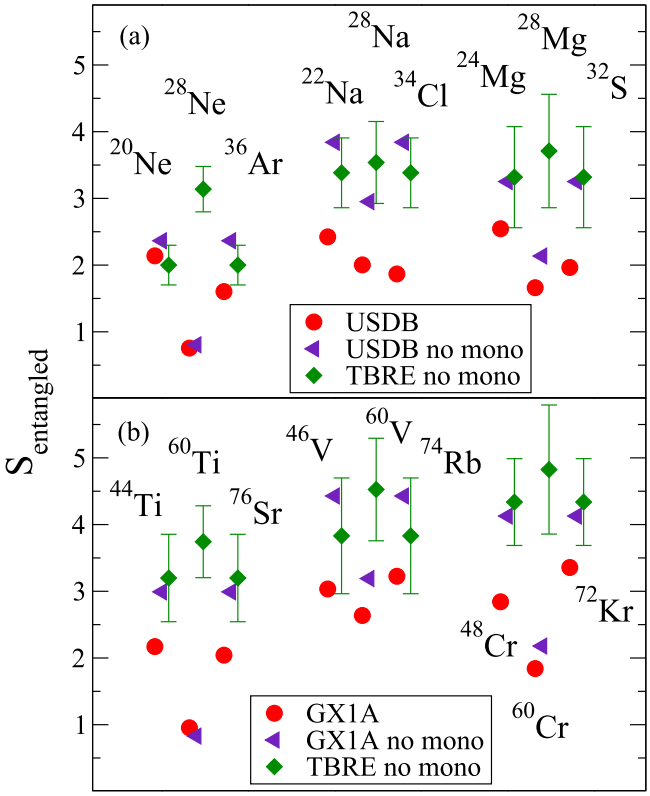

Figure 2. Ground state entanglement beyond $N = Z$. Here we compare nuclide triplets with the same dimensionalities (and thus the same maximum entanglement entropy), with the same number of protons/proton holes and neutrons/neutron holes; not all cases correspond to physical nuclides. Panel (a) is for *sd*-shell nuclides, while panel (b) is for *pf*-shell nuclides. Here USDB [20] is an empirical interaction for the *sd*-shell while GX1A [22–24] is for the *pf*-shell. We also show the average and standard deviation for interactions drawn from the two-body random ensemble (TBRE). Finally, 'no mono' means the single-particle energies and monopole interaction terms have been set to zero, thus eliminating any shell structure [18].

interaction [26]. In order to compare with past results, we restrict the space so as to follow the dimensionalities of figure 1. Thus we restrict protons to the *sd*-shell, while for neutrons the *sd*-shell and the $0f_{7/2}$ orbitals are filled and frozen, leaving only $0f_{5/2}$-$1p_{3/2}$-$1p_{1/2}$ as the active space for neutrons. Finally, we restrict ourselves to the same number of active protons and neutrons. Thus the nuclides correspond to ^{40}Ne, ^{42}Na, ^{44}Mg, and so on, through ^{56}Ar. These restrictions are chosen so that the dimensionalities are the same as in figure 1. While somewhat artificial–we do not claim all these correspond to physical nuclides–this nonetheless allows us to make a clean investigation into the entanglement. For ease of comparison, we include the USDB and USDB monopole-subtracted ('no mono') results for $N = Z$ nuclides, shifted over by $A = 20$ (so that ^{20,40}Ne are superimposed, etc). Again we see a low entanglement entropy, even lower than for the *sd*-shell examples in figure 1, although the 'no monopole' case shows much of this is driven by shell structure. Nonetheless, this provides evidence that the low entanglement for $N \neq Z$ nuclides persists for cross-shell spaces.

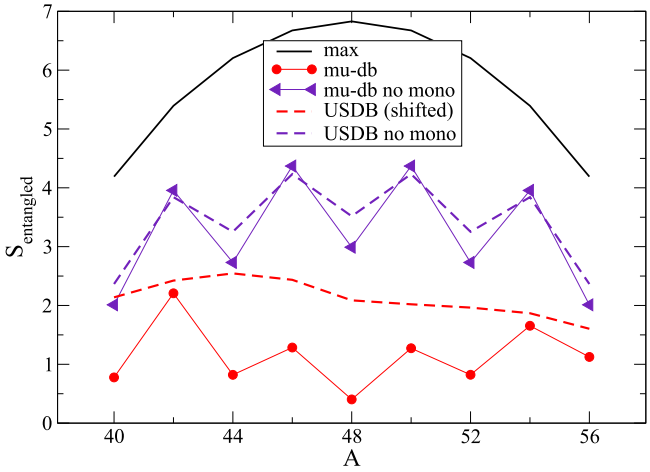

Figure 3. Entanglement entropies for nuclides in the *sd-pf* space, from ^{40}Ne through ^{56}Ar. See text for a detailed description of the model space, which is truncated so that the dimensionalities are the same as for $N = Z$ *sd*-shell nuclides in figure 1. Here 'mu-db' is the interaction of [26], while 'max' and 'no mono' mean the same as in figure 1. We also include for comparison *sd*-shell results from figure 1 (dashed lines), shifted by $A = 20$.

It is important to note that this is not simply isospin. Although we do not show it, for a given N and Z, states of different J and T nonetheless show very similar trends. In other words, this behavior is related to T_z, not T. In the next section, we investigate further.

4.3. Entanglement entropies of excited levels

In the previous results, we focused on ground state entanglement. Here we look at systems where we can fully diagonalize and compute the entanglement entropy across the spectrum.

In figure 4 we present the entanglement entropy for all levels for several nuclides computed with empirical interactions that give a good description of the data. Specifically we consider ^{20,28}Ne and ^{36}Ar, computed in the *sd*-shell with the USDB interaction [20], and ^{40}Ne computed in a truncated *sd-pf* space, computed with a cross-shell interaction [26]; for the latter, we restricted the valence protons to the *sd*-shell, and froze all neutrons in the *sd*-shell and in the $0f_{7/2}$ orbital, so that we have only two valence neutrons in the $0f_{5/2}$-$1p_{3/2}$-$1p_{1/2}$ orbitals. These choices are made so that all four cases have exactly the same dimensionalities. While each plot has a considerable scatter, there are a couple of noticeable features. The first is an overall curvature: on average, the entropy rises and then falls. The second feature is that the isospin-asymmetric nuclides, ^{28,40}Ne, are noticeably more asymmetric in the distribution of entropies, in particular the low entropy of the ground state as pointed out in the previous section.

To probe the origin of these behaviors, in figure 5 we recomputed the entropies for ^{20,28,40}Ne. In the top panels, figures 5(a)–(c), we set the single-particle energies and monopole interaction terms to zero. (Note that in such a scenario, there is a particle-hole symmetry, so that ^{36}Ar would be exactly the same as ^{20}Ne.) This has the effect of amplifying the asymmetry in all three cases. In the bottom panels, figures 5(d)–(f), we instead generated a random set of two-body matrix elements, and also removed the monopole interaction terms. Here the asymmetry vanishes, and the curvature for ^{20,28}Ne is much reduced. An important lesson we

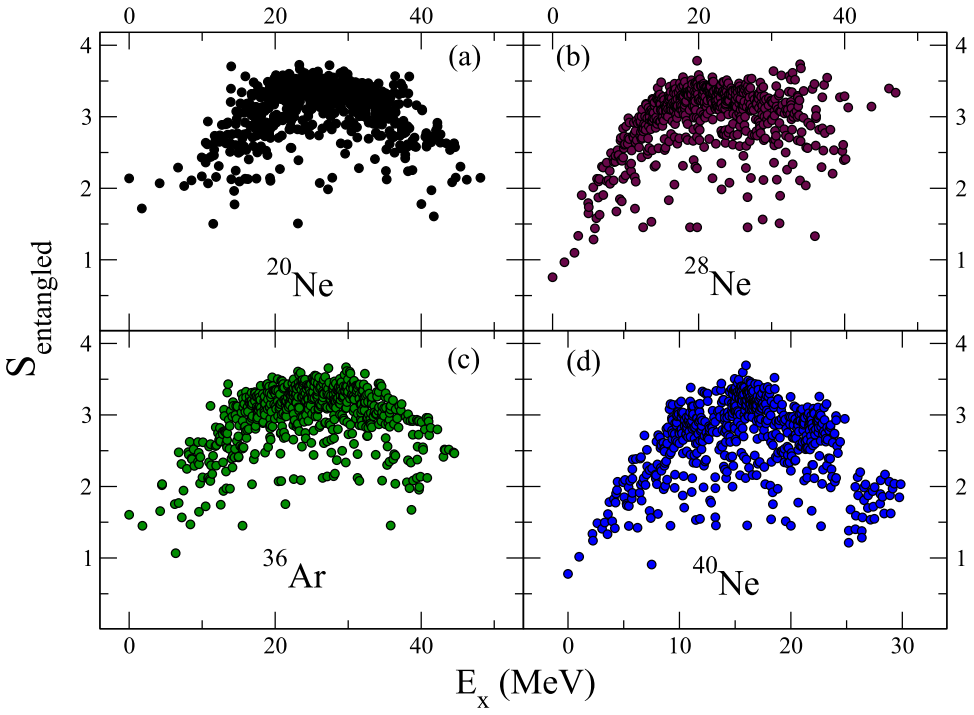

Figure 4. Entanglement entropies for all levels as a function of excitation energy E_x. Panels (a), (b), and (c) are computed in the *sd*-shell using the USDB interaction [20]. Panel (d) is computed in the *sd-pf* space, using the 'mu-db' interaction [26]; certain orbits are frozen in order to make the dimensions for this case the same as the other three cases. The maximum entanglement entropy is at the top of each plot.

learn is that the T_z dependence of the entropy appears to come out of the physical nuclear force, as it does not appear when using a randomly generated interaction.

5. Conclusions and acknowledgments

We have found that both schematic and realistic nuclear shell model Hamiltonians have low entanglement between the proton and neutron components of the wave function. This is particularly pronounced for states with high isospin. Part of the behavior is governed by the shell structure, which reduces the effective dimensionality, but, by using random two-body matrix elements, we can establish that the low entropy also is a feature of typical nuclear forces. While we have spent considerable effort to construct toy models to understand this behavior, so far none of them have provided convincing illumination.

A low entanglement means that one can get a good approximation to a wave function using a much smaller subset of basis states. This is the driving idea between the density matrix renormalization group methods [27–29], which have only been used sporadically in nuclear structure physics [12, 30–33], partitioning on orbitals rather than between protons and neutrons. Closer to the present work is the proton-neutron singular-value decomposition analysis of shell model wave functions [34, 35]; ironically, the latter studies focused on $N \approx Z$ nuclides. One happy conclusion from our work presented here is that reduced basis methods,

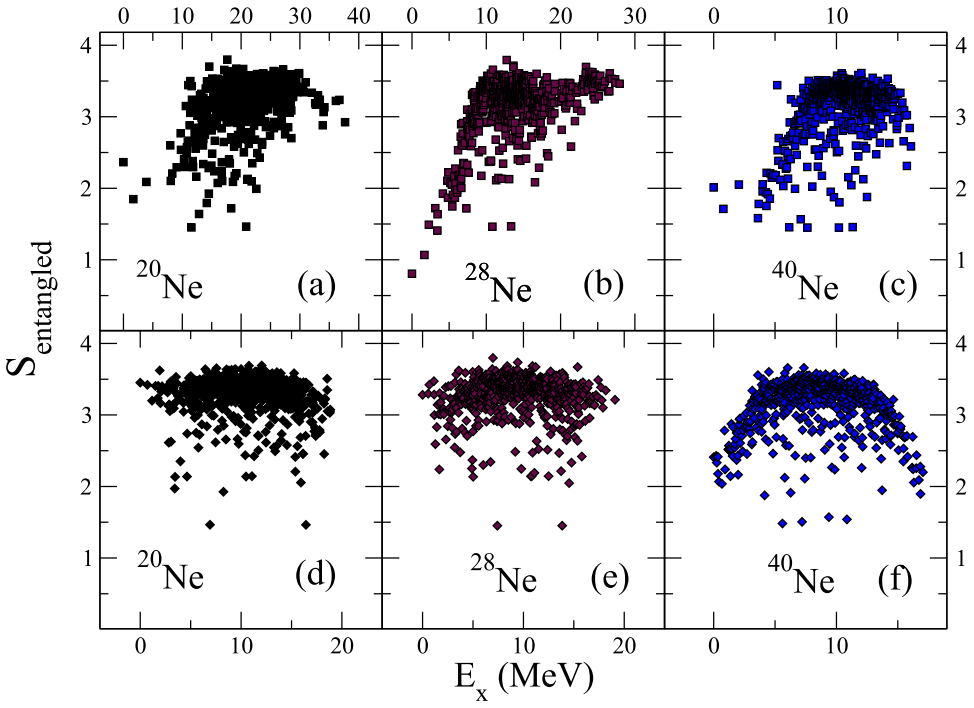

Figure 5. Entanglement entropies for all levels as a function of excitation energy E_x. The top panels, (a)–(c), are computed with realistic interactions (USDB for panels (a) and (b), and 'mu-db' for panel (c)) but with all single-particle energies and monopole interaction terms set to zero, so as to remove shell effects. The bottom panels, (d)–(f), correspond to the same nuclides, but with a random two-body interaction. The maximum entanglement entropy is at the top of each plot.

justified by low entanglement [36], may be even more effective for high-isospin nuclides, such as heavy nuclei, where the need for dimensional reduction is the greatest. We have made progress in a systematic implementation of this idea and will present results soon.

This material is based upon work supported by the U.S. Department of Energy, Office of Science, Office of Nuclear Physics, under Award Number DE-FG02-03ER41272, and by the Office of High Energy Physics, under Award No. DE-SC0019465, and by Lawrence Livermore National Laboratory under Contract DE-AC52-07NA27344, with support from the ACT-UP award.

Data availability statement

The data cannot be made publicly available upon publication because they are not available in a format that is sufficiently accessible or reusable by other researchers. The data that support the findings of this study are available upon reasonable request from the authors.

Appendix. Schematic interactions

Schematic interactions are well-known to capture many features of nuclear structure and have long been used in nuclear physics [2, 16, 25]. For completeness, we summarize them here.

- Quadrupole–Quadrupole (QQ): we construct a quadrupole operator

$$\hat{Q}_{2M,TM_T} = \sum_{ab} Q_{ab}[\hat{c}_a^\dagger \otimes \tilde{c}_b]_{2M,TM_T}, \tag{A.1}$$

where a, b are indices for single-particle orbits defined by n, l, j; $[\cdot\otimes\cdot]_{JM,TM_T}$ indicates coupling by Clebsch–Gordan coefficients up to total angular momentum J (here $J=2$) and z-component M and total isospin T and third component M_T; $\hat{c}_a^\dagger$ creates a particle in orbit a, $\tilde{c}_b$ is a time-reversed destruction operator [37] for a particle in orbit b; and finally the reduced matrix elements [37] of the quadrupole operator (which we compute in a harmonic-oscillator basis)

$$Q_{ab} = \langle a||r^2Y_2||b\rangle, \tag{A.2}$$

where $Y_{lm}(\theta, \phi)$ is a spherical harmonic. The quadrupole–quadrupole Hamiltonian is

$$V_{QQ}[\hat{Q} \otimes \hat{Q}]_{00,00}, \tag{A.3}$$

where V_{QQ} is the strength of the interaction and is taken <0 to make it attractive; because we only focus on the wave functions and not the energies, the magnitude of V_{QQ} is unimportant here. For our calculations we considered only the isoscalar ($T=0$) QQ interaction.

- Pairing. The pairing operator is

$$\hat{P}^\dagger_{TM_T} = \sum_a \sqrt{2j_a+1}\,[\hat{c}_a^\dagger \otimes \hat{c}_a^\dagger]_{00,TM_T}, \tag{A.4}$$

where j_a is the angular momentum of orbital a. The pairing Hamiltonian is

$$G\sum_{M_T}(-1)^{T-M_T}\hat{P}^\dagger_{TM_T}\hat{P}_{TM_T}, \tag{A.5}$$

where G is the strength of the pairing Hamiltonian, and is taken <0 to make attractive. Here $T=1$ yields isovector pairing and $T=0$ isoscalar pairing.

ORCID iDs

Calvin W Johnson https://orcid.org/0000-0003-1059-7384
Oliver C Gorton https://orcid.org/0000-0003-3643-9640

References

[1] Talmi I 1993 *Simple Models of Complex Nuclei* (Boca Raton: CRC Press)
[2] Ring P and Schuck P 2004 *The Nuclear Many-body Problem* (New York: Springer Science & Business Media)
[3] Bahri C, Rowe D J and Wijesundera W 1998 Phase transition in the pairing-plus-quadrupole model *Phys. Rev.* C **58** 1539–50
[4] Rowe D J 2000 Quasi-dynamical symmetry: a new use of symmetry in nuclear physics *The Nucleus* (Boston, MA: Springer) pp. 379–95
[5] Bahri C and Rowe D J 2000 SU(3) quasi-dynamical symmetry as an organizational mechanism for generating nuclear rotational motions *Nucl. Phys.* A **662** 125–47
[6] Amico L, Fazio R, Osterloh A and Vedral V 2008 Entanglement in many-body systems *Rev. Mod. Phys.* **80** 517–76
[7] Schroeder D V 2017 Entanglement isn't just for spin *Am. J. Phys.* **85** 812–20
[8] Horodecki R, Horodecki P, Horodecki M and Horodecki K 2009 Quantum entanglement *Rev. Mod. Phys.* **81** 865–942

[9] Strauch F W 2016 Resource letter QI-1: quantum information *Am. J. Phys.* **84** 495–507
[10] Robin C, Savage M J and Pillet N 2021 Entanglement rearrangement in self-consistent nuclear structure calculations *Phys. Rev.* C **103** 034325
[11] Kruppa A T, Kovács J, Salamon P, Legeza Ö and Zaránd G 2022 Entanglement and seniority *Phys. Rev.* C **106** 024303
[12] Tichai A, Knecht S, Kruppa A T, Legeza Ö, Moca C P, Schwenk A, Werner M A and Zarand G 2022 Combining the in-medium similarity renormalization group with the density matrix renormalization group: shell structure and information entropy arXiv:2207.01438
[13] Horoi M, Zelevinsky V and Brown B A 1995 Chaos versus thermalization in the nuclear shell model *Phys. Rev. Lett.* **74** 5194–7
[14] Zelevinsky V, Horoi M and Brown B A 1995 Information entropy, chaos and complexity of the shell model eigenvectors *Phys. Lett.* B **350** 141–6
[15] Volya A and Zelevinsky V 2003 Invariant correlational entropy as a signature of quantum phase transitions in nuclei *Phys. Lett.* B **574** 27–34
[16] Brussard P J and Glaudemans P W M 1977 *Shell-Model Applications in Nuclear Spectroscopy* (Amsterdam: North-Holland Publishing Company)
[17] Brown B A and Wildenthal B H 1988 Status of the nuclear shell model *Annu. Rev. Nucl. Part. Sci.* **38** 29–66
[18] Caurier E, Martinez-Pinedo G, Nowacki F, Poves A and Zuker A P 2005 The shell model as a unified view of nuclear structure *Rev. Mod. Phys.* **77** 427–88
[19] Johnson C W, Ormand W E and Krastev P G 2013 Factorization in large-scale many-body calculations *Comput. Phys. Commun.* **184** 2761–74
[20] Brown B A and Richter W A 2006 New USD hamiltonians for the *sd* shell *Phys. Rev.* C **74** 034315
[21] Johnson C W, Bertsch G F and Dean D J 1998 Orderly spectra from random interactions *Phys. Rev. Lett.* **80** 2749–53
[22] Honma M, Otsuka T, Brown B A and Mizusaki T 2002 Effective interaction for pf-shell nuclei *Phys. Rev.* C **65** 061301
[23] Honma M, Otsuka T, Brown B A and Mizusaki T 2004 New effective interaction for pf-shell nuclei and its implications for the stability of the $N = Z = 28$ closed core *Phys. Rev.* C **69** 034335
[24] Honma M, Otsuka T, Brown B A and Mizusaki T 2005 Shell-model description of neutron-rich pf-shell nuclei with a new effective interaction GXPF1 *Eur. Phys. J.* A **25** 499–502
[25] Bohr A and Mottelson B R 1998 *Nuclear Structure* (Singapore: World Scientific) vol. 1
[26] Iwata Y, Shimizu N, Otsuka T, Utsuno Y, Menéndez J, Honma M and Abe T 2016 Large-scale shell-model analysis of the neutrinoless $\beta\beta$ decay of ^{48}Ca *Phys. Rev. Lett.* **116** 112502
[27] White S R 1992 Density matrix formulation for quantum renormalization groups *Phys. Rev. Lett.* **69** 2863–6
[28] White S R 1993 Density-matrix algorithms for quantum renormalization groups *Phys. Rev.* B **48** 10345–56
[29] Schollwöck U 2005 The density-matrix renormalization group *Rev. Mod. Phys.* **77** 259–315
[30] Dukelsky J, Pittel S, Dimitrova S S and Stoitsov M V 2002 Density matrix renormalization group method and large-scale nuclear shell-model calculations *Phys. Rev.* C **65** 054319
[31] Rotureau J, Michel N, Nazarewicz W, Płoszajczak M and Dukelsky J 2006 Density matrix renormalization group approach for many-body open quantum systems *Phys. Rev. Lett.* **97** 110603
[32] Thakur B, Pittel S and Sandulescu N 2008 Density matrix renormalization group study of ^{48}Cr and ^{56}Ni *Phys. Rev.* C **78** 041303
[33] Legeza Ö, Veis L, Poves A and Dukelsky J 2015 Advanced density matrix renormalization group method for nuclear structure calculations *Phys. Rev.* C **92** 051303
[34] Papenbrock T and Dean D J 2003 Factorization of shell-model ground states *Phys. Rev.* C **67** 051303
[35] Papenbrock T, Juodagalvis A and Dean D J 2004 Solution of large scale nuclear structure problems by wave function factorization *Phys. Rev.* C **69** 024312
[36] Weinstein M, Auerbach A and Chandra V R 2011 Reducing memory cost of exact diagonalization using singular value decomposition *Phys. Rev.* E **84** 056701
[37] Edmonds A R 1996 *Angular Momentum in Quantum Mechanics* (Princeton: Princeton University Press)